Motional Stark Effect Polarimetry for the Current Profile Diagnostic in DIII-D*

UCRL-JC--103464
DE90 012071

D. Wróblewski
Lawrence Livermore National Laboratory, Livermore, CA 94550

K. H. Burrell, L. Lao, P. Politzer, and W. P. West
General Atomics, San Diego, CA 92158

Abstract

Motional Stark effect produces large net linear polarization of hydrogenic beam emissions. Measurement of the polarization direction permits to determine the local magnetic field pitch angle. Design of a single point, spatially scannable, high-sensitivity polarimeter installed on DIII-D is described. Excellent signal-to-noise ratio with good temporal and spatial resolution was obtained in preliminary measurements of magnetic field pitch angle.

MASTER

DISTRIBUTION OF THIS DOCUMENT IS UNLIMITED

1. Introduction

Spectroscopic diagnostics of the poloidal magnetic field in a tokamak are based on the polarimetry of spectral lines. When the polarization of a line is due to the Zeeman effect, a fundamental difficulty is associated with the fact that the Zeeman effect splitting is usually smaller (as for the neutral beam emissions[1,2]) or much smaller (for emissions of thermalized impurities[3,4]) than the line width. This results in almost prohibitively small polarization effects which need to be measured to provide a reasonable accuracy of the poloidal field determination. Recent PBX-M results indicate that this problem may be avoided by the use of H_α line emitted from a neutral beam.[5] Hydrogen exhibits a linear and thus unusually strong Stark effect (splitting and shift of atomic energy levels in an external electric field). In the case of high energy hydrogen or deuterium beam in a tokamak, the line structure is dominated by the motional Stark effect due to the Lorentz electric field $\mathbf{E} = \mathbf{v} \times \mathbf{B}$, where $\mathbf{v}$ is the beam velocity, and $\mathbf{B}$ is the total magnetic field.

Stark effect produces splitting of the Balmer-α line (H_α/D_α, λ_0=6562 Å, transition $n = 3 \rightarrow 2$) into 15 components, only 9 of which have appreciable intensity.[6] These components are divided into two polarization groups. The π lines (transitions for which Δm=0) are linearly polarized parallel to $\mathbf{E}$ (having no intensity when observed along $\mathbf{E}$), and the σ lines ($\Delta m = \pm 1$) are polarized perpendicular to $\mathbf{E}$ when viewed perpendicular to $\mathbf{E}$ and are unpolarized when viewed along $\mathbf{E}$. Here, m is the projection of the total orbital momentum on the electric field direction. In DIII-D, Doppler shifted beam emissions are observed at full, 1/2, and 1/3 beam energy, corresponding to the beam molecular composition.[7] For each beam energy component, three components of H_α line may be resolved. The central peak is a blend of three Stark σ-components and each of the side peaks is a blend of three Stark π-components. Typical wavelength separation of σ and π manifolds is 5 Å.

The magnetic field pitch angle measurement utilizes the fact that the σ–components are polarized in the direction perpendicular to the local electric field and the measurement of polarization direction allows to determine the local magnetic field pitch angle. Large wavelength separation between σ and π features results in an excellent signal–to–noise ratio.

The Balmer–β (H_β) line ($\lambda_0 = 4861.3\AA$, transition $n = 4 \rightarrow 2$) has two σ and two π manifolds. Their wavelength separation is not as pronounced as for H_α and the fractional linear polarization in the center of the σ component is slightly smaller for H_β than for H_α. As the detection efficiency is expected to be somewhat better at the H_β wavelength, this line may provide a measurement of comparable quality.

2. Geometry of the measurement

DIII–D tokamak is equipped with eight high power neutral beams injected almost tangentially on the machine midplane from four toroidal locations — Figure 1. Thus, in the absence of plasma current, the motional electric field is vertical. Deviation from the vertical direction is produced by the electric field component due to poloidal (vertical) magnetic field and either radial component of the beam velocity (for observation in the radial direction), or toroidal component of the beam velocity (for observation tangential to the toroidal direction). The diagnostic described here employes an almost tangential view close to the machine midplane, analogous to the one used by the tangential CER system[7]. This geometry has several advantages:

(1). The viewing line, at the region of intersection with the beam, is nearly tangential to the flux surfaces, therefore providing a reasonable localization of the measurement in the major radial direction. The beam cross–section is approximately 50 cm high and 10 cm wide.

(2). The available observation ports have sufficient aperture for a multi-sightline system covering R=150 cm—230 cm (tokamak major radius is 164 cm, the plasma outer edge is typically at about 230 cm).

(3). The angle between the sightlines and the neutral beam yields a sufficiently large Doppler shift to resolve the beam emissions from the thermal (plasma edge) emission, and to resolve beam energy components.

The relation between measured polarization direction and actual magnetic field pitch angle depends on the observation direction with respect to the beam velocity and the magnetic field. In general, a projection of the pitch angle on the plane perpendicular to the direction of observation is measured. With the beam velocity on the midplane, at angle α to B_T, and the observation direction at angle Ω to B_T and at angle θ to the vertical direction, the measured tilt angle of the polarization vector, γ_m, is given by:

$$tg\gamma_m = -\frac{B_V cos(\alpha+\Omega)}{B_V cos\theta sin(\alpha+\Omega) - sin\theta(B_R cos\alpha - B_T sin\alpha)}, \qquad (1)$$

where B_V, B_R, and B_T are the vertical, radial, and toroidal components of the magnetic field. In the present set-up, $\theta \simeq$93 deg and

$$tg\gamma_m \simeq \frac{B_V cos(\alpha+\Omega)}{B_R cos\alpha - B_T sin\alpha} \simeq -\frac{B_V cos(\alpha+\Omega)}{B_T sin\alpha}. \qquad (2)$$

Thus, the tangential observation results in a reduction of the measured tilt angle with respect to the actual magnetic field pitch angle. In the present geometry, the reduction factor is about 0.9 for the "left" (more tangential) neutral beam and 0.6–0.8 for the "right" beam, depending on the spatial position.

3. Polarimeter

The instrument consists of polarizer head (mounted on the machine port), fiber optic link, wavelength filter, photomultiplier detector, and lock-in amplifiers (all placed outside the machine enclosure).

3.1. Polarizer

The polarization measurement is based on a high frequency polarization modulation of the beam emission and lock-in detection of the signal.[5,8,9] A photoelastic modulator (PEM) is the main component of the polarizer. This device serves as an oscillating wave-plate with the retardation varying from $-\lambda/2$ to $+\lambda/2$, and produces fast rotation of the direction of linear polarization of transmitted light. PEM is followed by a stationary linear polarizer which transforms the polarization direction modulation into intensity modulation.

For the linear polarization direction measurement, the optimum system consists of two PEM's working at slightly different frequencies. The first modulator optical axis is placed along the tokamak vertical axis (z-axis), the second modulator axis is at 45 deg to the z-axis. The modulator frequencies are 42 kHz and 47 kHz. The modulators are followed by a stationary linear polarizer oriented at 22.5 deg to the z-axis. The light intensity behind the polarizer is given by:

$$2S = (I_\sigma + I_\pi) + \frac{(I_\sigma - I_\pi)}{\sqrt{2}}[-cos\delta_1 sin2\gamma + cos\delta_2 cos2\gamma - sin\delta_1 sin\delta_2 sin2\gamma], \quad (3)$$

where $I_\sigma(\lambda)$ and $I_\pi(\lambda)$ are wavelength dependent intensities of σ and π manifolds, δ_1 and δ_2 are the time dependent retardations produced by the first and the second PEM at frequencies ω_1 and ω_2, respectively.

There is no coupling between the modulations of the transmitted signal at frequencies $2\omega_1$ and $2\omega_2$. (There is a coupling, resulting from the last term of Eq. 3, between the modulations at the fundamental frequencies). With the same retardation amplitude, ϕ_0, for both modulators, the modulation amplitudes at $2\omega_1$ and $2\omega_2$ are given, respectively, by:

$$S_{ac1} = \frac{I_\sigma - I_\pi}{\sqrt{2}} J_2(\phi_0) sin2\gamma, \quad (4)$$

and

$$S_{ac2} = -\frac{I_\sigma - I_\pi}{\sqrt{2}} J_2(\phi_0) cos2\gamma. \quad (5)$$

Ratio of the modulation amplitudes gives:

$$\frac{S_{ac1}}{S_{ac2}} = -tg2\gamma. \tag{6}$$

Thus, in this arrangement, the result of polarization direction measurement does not depend on the wavelength and details of the line profile shape. The signal-to-noise ratio depends on the wavelength separation of σ and π components and is the largest at the wavelength at which $I_\sigma - I_\pi$ has maximum, i.e. at the center of σ manifold.

Figure 2 shows the polarizer head. The light is collected by about 6 cm diameter lens, then collimated and transmitted through the two PEMs and a polarizing cube. The third lens focuses the radiation on a 1 mm diameter optical fiber which carries the light outside the machine enclosure. Note that the use of only one fiber results in the loss of half of the radiation. Another focusing lens and a second fiber is placed perpendicular to the optical axis of the set-up to retrieve this radiation. The signals carried by both fibers are identical except for 180 degree shift in the phase of high-frequency intensity modulation.

The demagnification of this optical system is about 20 which gives the spatial resolution in the plasma of about 2 cm. Some additional degradation of spatial resolution is due to line-of-sight integration over the beam width.

The polarizer head views the plasma through a glass window on a tangential port located about 13 cm below the machine midplane. It is mounted at a small angle to the horizontal plane in such a way that the sightline crosses the 30 Left neutral beam in the vicinity of the machine midplane. The optics is placed in a precision tilt mechanism that allows for an accurate and reproducible positioning of the sightline-beam intersection point at 17 different major radii.

3.2. Wavelength filter

The intensity modulated radiation is transmitted to the interference filter spectrometer. This set-up houses the collimating optics, narrow bandpass (3 Å) interference filter and photomultiplier detectors.

The peak transmission wavelength of the filter may be decreased by tilting the filter. To facilitate a fast wavelength scan the filter is mounted on motor driven tilt stage with a position monitor. The position of maximum polarization signal, corresponding to the center of σ-manifold, depends on the Doppler shift (and thus, beam energy and sightline) and may be empirically determined during one beam and plasma pulse.

The light emerging from two optical fibers remains geometrically separated in the spectrometer but the wavelength response is the same for both channels. In the last stage of the set-up, the light is focused on two photomultiplier tubes.

3.3. Signal analysis

The photomultiplier signals are filtered and amplified by two lock-in amplifiers referenced to the PEMs phase and frequency. Differential input option of the lock-in amplifiers allows to add the signals from two photomultipliers and to use only one amplifier for a given modulation frequency. The lock-in amplifiers output signals proportional to the magnitude of the modulation at a given frequency. These signals are digitized and stored in the DIII-D data base. As shown above, the ratio of these signals is a function of the pitch angle, γ_m.

3.4. Calibrations

All the linear polarization analyzers share a rather serious drawback that the polarizing optics must be very accurately aligned with respect to the reference direction of polarization tilt measurement (in this case, the tokamak midplane). The accuracy of this alignment must be better than the required accuracy of the pitch angle measurement ($\leq$ 0.5 deg).

Two stage angle calibration is performed. In the gain calibration, a laboratory light source is used, a linear polarization filter is placed in front of the polarizer head and polarimeter signals are measured as a function of the polarizer angular position. The offset angle (angle measured for zero tokamak magnetic field pitch angle) is determined *in situ* by measuring the polarization tilt angle in the absence of plasma current. This kind of data is obtained by firing the neutral beam into machine with only the toroidal field coils activated. Another calibration involves measurement of the tilt angle at the plasma edge. The offset is obtained by comparing the measured value with the result of magnetic probe measurements and equilibrium calculations. A rather large value of offset angle, about 5 degrees, is obtained in these measurements. Mechanical misalignment of the polarizer may be one source of the offset. There is also a possibility of appreciable Faraday rotation effect in the polarizer head optics. It is estimated that the toroidal field component along the polarizer optical axis may produce rotation of the linear polarization direction of 2-3 degrees.

An accurate determination of the measurement geometry, i.e. angles α, Ω, and θ in Eq. 1, and of the radial position of the measurement volume (intersection of the instrument sightline with the neutral beam) is also of crucial importance in the interpretation of experimental data. This information is obtained by in vessel calibration in which the instrument is backlighted and positions of all sightlines are measured with respect to the machine fiducial points.

4. Preliminary results

The motional Stark effect polarimeter has been successfully operated in DIII-D. Strong polarization signals are routinely obtained at densities of up to 10^{14} cm^{-3}, and at up to 40 cm from the plasma edge. With the time resolution (amplifiers response time) of 10 ms, the noise level of the tilt angle measurement is at the level of 0.1-0.2 degree, i.e. less then 3 % of the measured angle.

Figure 3 shows an example of polarimeter data obtained for a double null divertor discharge with total current 1 MA and toroidal field 1.2 Tesla. The polarization measurement is obtained at major radius R=192 cm, the plasma edge is at R=225 cm (on the midplane), and the plasma magnetic axis is at R≃166 cm. The data were taken during the plasma current ramp–up which is reflected by increase of the measured pitch angle. The figure also shows the soft x–ray diagnostic data from one central and one edge sightline, which demonstrate sawtooth activity in the plasma center. Sawtooth inversion radius deduced from soft x–ray signals is at about R=181 cm. The magnetic field pitch angle signal seems to be correlated with the sawtooth period and indicates flattening of the current profile (decrease of the pitch angle) after the sawtooth crash, and peaking of the current profile before the crash. This is in qualitative agreement with reconnection model of sawtooth. The response time of the polarimeter (integration time of lock–in amplifiers) is in this case about 10 ms, much slower than the crash time observed by the soft x–ray diagnostic.

The result of motional Stark effect polarization measurement will be incorporated into the magnetic equilibrium code to provide a constraint on the calculated current density profile (or the safety factor on axis, q(0)). The code employs data from a number of magnetic field probes placed on the plasma periphery. Initial attempt to determine q(0) from the data presented in Figure 3 resulted in q(0)≃1.05 after the sawtooth crash, and q(0)≃0.95 before the crash. The accuracy of this result is about 0.2, with the main error source being the uncertainty of offset angle measurement.

Acknowledgements

We would like to thank Dr. Hirotaka Kubo (JAERI) for his help in data analysis.

This work is supported by USDOE Contracts W–7405–ENG–48 and DE–AC03–89ER51114.

Figure Captions

Figure 1. Top view of DIII-D showing the neutral beam geometry and spatial coverage of the polarimeter (shaded area). Either of the beams from 30 deg. beamline may be employed in the measurement.

Figure 2. Polarizer head design.

Figure 3. Example of a plasma shot with the polarimeter data and deduced magnetic field tilt angle.

References

1. K. McCormick, F. X. Soldner, D. Eckhartt, F. Leuterer, H. Murmann, *et al.*, *Phys. Rev. Lett* **58**, 491 (1987).

2. W. P. West, D. M. Thomas, J. S. deGrassie, and S. B. Zheng, *Phys. Rev. Lett.* **58**, 2758 (1987).

3. D. Wróblewski, L. K. Huang, H. W. Moos, and P. E. Phillips, *Phys. Rev. Lett.* **61**, 1724 (1988).

4. D. Wróblewski and H. W. Moos, *Rev. Sci. Instrum.* **57**, 2029 (1986).

5. F. M. Levinton, *et al.*, *Phys. Rev. Lett.* **63**, 2060 (1989).

6. H. A. Bethe, and E. E. Salpeter, *Quantum Mechanics of One- and Two-Electron Atoms*, Springer-Verlag, Berlin, 1957.

7. R. P. Seraydarian, K. H. Burrell, and R. J. Groebner, *Rev. Sci. Instrum.* **59**, 1530 (1988).

8. J. C. Kemp, *Polarized Light and its Interaction with Modulating Devices - a Methodology Review*, Hinds International, 1987.

9. D. Wróblewski, L. K. Huang, and H. W. Moos, *Rev. Sci. Instrum.* **59**, 2341 (1988).

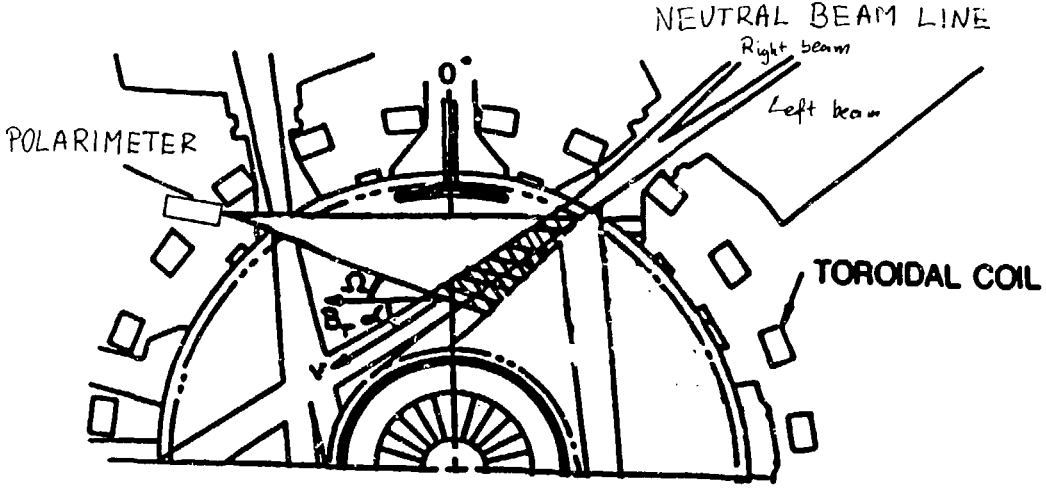
NEUTRAL BEAM LINE
Right beam
Left beam
POLARIMETER
TOROIDAL COIL

Fig. 1

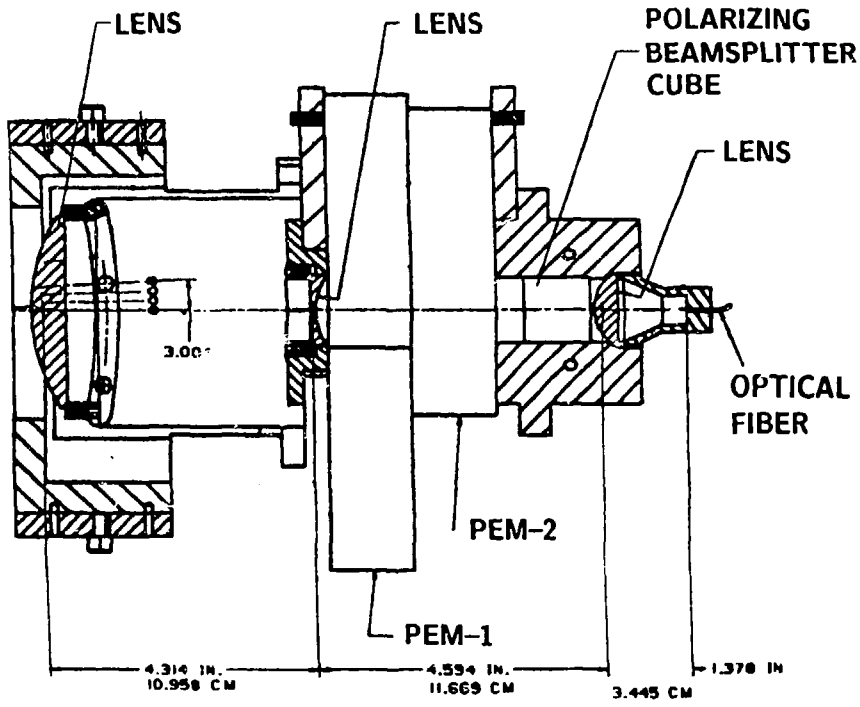
LENS
LENS
POLARIZING
BEAMSPLITTER
CUBE
LENS
OPTICAL
FIBER
PEM–2
PEM–1
4.314 IN.
10.958 CM
4.594 IN.
11.669 CM
3.445 CM
1.378 IN

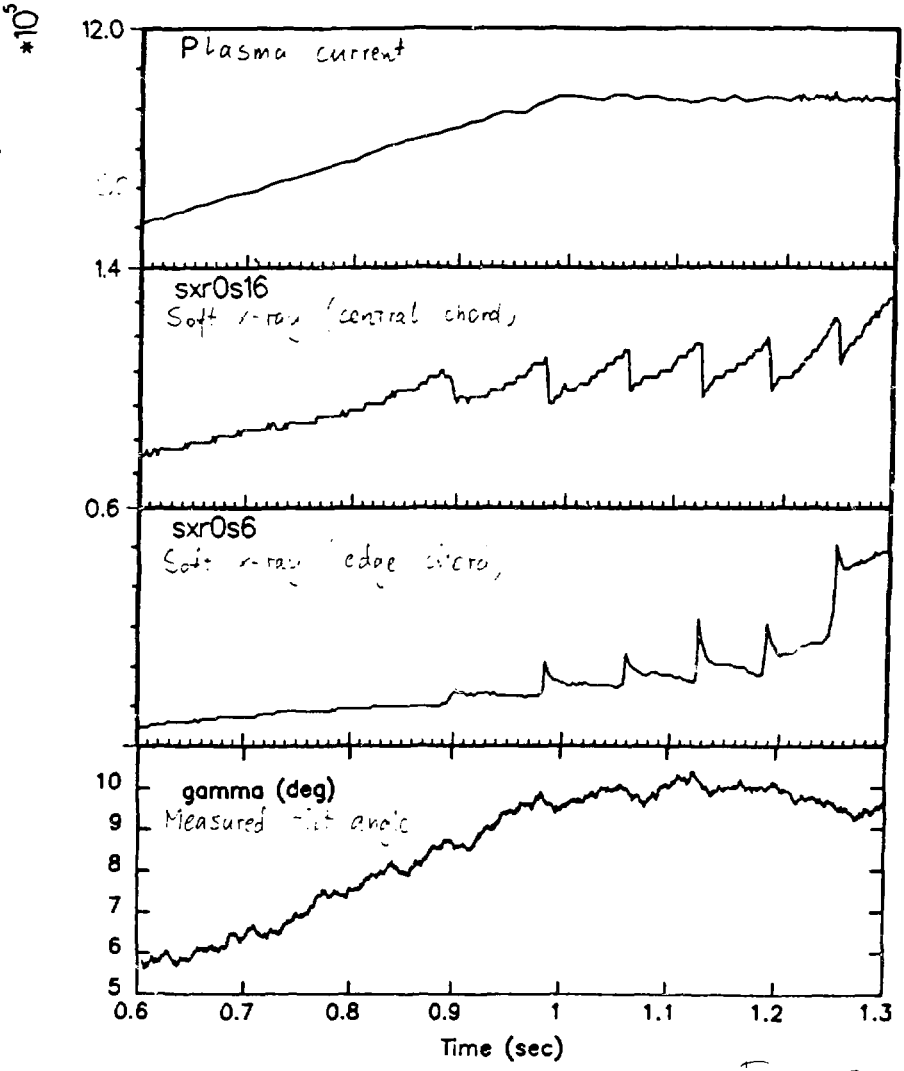
*10^5
12.0
Plasma current
1.4
sxr0s16
Soft x-ray (central chord)
0.6
sxr0s6
Soft x-ray edge micro
10
9
8
7
6
5
gamma (deg)
Measured tilt angle
0.6
0.7
0.8
0.9
1
1.1
1.2
1.3
Time (sec)

Fig. 3